

# A Capsule Network-based Model for Learning Node Embeddings

Dai Quoc Nguyen<sup>1</sup> and Tu Dinh Nguyen<sup>2</sup> and Dat Quoc Nguyen<sup>3</sup> and Dinh Phung<sup>4</sup>

**Abstract.** In this paper, we focus on learning low-dimensional embeddings of entity nodes from graph-structured data, where we can use the learned node embeddings for a downstream task of node classification. Existing node embedding models often suffer from a limitation of exploiting graph information to infer plausible embeddings of unseen nodes. To address this issue, we propose Caps2NE—a new unsupervised embedding model using a network of two capsule layers. Given a target node and its context nodes, Caps2NE applies a routing process to aggregate features of the context nodes at the first capsule layer, then feed these features into the second capsule layer to produce an embedding vector. This embedding vector is then used to infer a plausible embedding for the target node. Experimental results for the node classification task on six well-known benchmark datasets show that our Caps2NE obtains state-of-the-art performances.

## 1 Introduction

Numerous real-world and scientific data are represented in forms of graphs, e.g. data from knowledge graphs, recommender systems, social and citation networks as well as telecommunication and biological networks [2, 5]. In general, a graph can be viewed as a network of nodes and edges, where nodes correspond to individual entities and edges linking the nodes encode relationships among those entities, e.g. in modeling text classification on citation networks, each document is treated as a node, and a citation link between two documents is treated as an edge [30].

Recent years have witnessed many successful downstream applications of utilizing the graph-structured data such as for improving information extraction and text classification systems [15], traffic learning and forecasting [6] and for advertising and recommending relevant items to users [31, 29]. This is largely boosted by a surge of methodologies that learn embedding representations to encode structural information about the graphs [4]. One of the most important tasks in representation learning on graphs is to learn low-dimensional embedding vectors of entity nodes [12, 33]. These embedding vectors can then be used in a downstream task such as node classification, i.e. using the learned node embeddings as features to train a classifier for predicting node labels [11].

A simple and effective approach to learn node embeddings is to treat each node as a word token and each graph as a text collection, and then apply a word embedding model such as Word2Vec [20].

For example, DeepWalk [23] generates many unbiased random walks starting from each node, and then uses these walks as sequences of nodes (i.e. equivalent to sentences of words) to train a Word2Vec model. LINE [26] follows DeepWalk and introduces the node importance, in which each node has a different weight to each of its neighbors, where the weight can be pre-defined by algorithms such as PageRank [22]. Node2Vec [9] extends DeepWalk by introducing a biased random walk approach which explores diverse neighborhoods of a given node with a trade-off between breadth-first and depth-first sampling strategies. DDRW [17] jointly trains a DeepWalk model with a Support Vector Classification [8] in a supervised manner.

Some recent work has also investigated effects of deep neural networks to the node classification task, e.g., SDNE [28] and GCN—Graph Convolutional Network [15]. The autoencoder-based supervised model SDNE is introduced to preserve the local and global graph structures. GCN is another supervised model using a variant of convolutional neural networks [16], which makes use of layer-wise propagation to exploit features such as profile information and text attributes from the neighbors of a given node.

It is worth noting that existing approaches such as DeepWalk, LINE, Node2Vec, SDNE and GCN learn the embeddings of all nodes from a fixed graph structure, i.e. they can only classify nodes that are already observed in the graph during training. This is known as the *transductive* setting. However, in many cases such as operating on evolving graphs and constantly encountering unseen nodes, it would be better to have an *inductive* setting where a part of the graph is used to train the node embedding model, and the trained model can be then used to infer embeddings for unseen/new nodes, e.g. the ones in the remaining part of the graph [30]. Compared to the *transductive* setting, the *inductive* setting is particularly difficult because of requiring the ability to align newly observed nodes to the existing learned node embeddings [11].

There are embedding models proposed to work on both transductive and inductive settings such as EP-B [7] and GCN-based models GraphSAGE [11] and Graph Attention Network [27]. EP-B is proposed to explore the embedding representations of attributes, such as text and continuous features, associated with the nodes and their neighborhoods for inducing the embeddings of new nodes. GraphSAGE extends GCN by using node features and the neighborhood structures to generalize to new nodes. Graph attention network (GAT) follows LINE [26] to assign different weights to different neighbors of a given node, however, it learns these weights by exploring an attention mechanism technique [1]. It is important to note that GCN-based models shallowly aggregate feature information indirectly from nodes that are many hops away (i.e. non-neighbor nodes), by using multiple neural layers stacked on top of each other. Therefore, it is difficult for these GCN-based models

<sup>1</sup> Monash University, Australia, email: dai.nguyen@monash.edu

<sup>2</sup> Monash University, Australia, email: tu.dinh.nguyen@monash.edu

<sup>3</sup> The University of Melbourne, Australia, email: dqnguyen@unimelb.edu.au

<sup>4</sup> Monash University, Australia, email: dinh.phung@monash.edu

to infer plausible embeddings for new nodes especially when their neighbors are also unseen during training.

In this paper, we present Caps2NE—a new unsupervised embedding model that adapts capsule network [24] to unsupervisedly learn node embeddings. Here, our Caps2NE aims to capture context nodes many hops away from the random walks to predict a target node. More specifically, Caps2NE consists of two capsule layers with connections from the first to the second layer, but no connections within layers. The first layer uses groups of neurons as capsules to encapsulate corresponding context nodes and also exploits feature information of these context nodes. A routing process is used to aggregate the feature information from capsules in the first layer to only one capsule in the second layer. Then the second layer outputs a continuous vector which is used to infer an embedding for the target node. *It is important to note that encapsulating the context nodes into corresponding capsules aims to preserve node properties (e.g., relative positions, orientations and poses) more efficiently. And then the routing process can generate high-level features which are effective to infer plausible node embeddings not only for present nodes, but also for newly unseen nodes even when their neighbors are unseen during training. Our main contributions are as follows:*

- We introduce a novel use of the capsule network to learn node embeddings in graph-structured data. Our proposed model Caps2NE not only works advantageously in the transductive setting, but also can effectively infer the embeddings of the new nodes in the inductive setting.
- We conduct extensive experiments to evaluate the performance of Caps2NE on well-known benchmark datasets: CORA, CITESEER [25] and PUBMED [21] with node features. The experimental results for both the transductive and inductive settings show that our Caps2NE outperforms previous state-of-the-art unsupervised and supervised methods on CORA and CITESEER, and also obtains competitive performances on PUBMED.
- We also provide experiments for the transductive setting on PPI [3], POS [19] and BLOGCATALOG [32] without node features. Our Caps2NE achieves top performances on these three datasets.

## 2 The proposed Caps2NE

This section presents our Caps2NE model. In particular, we detail how to sample data from an input graph, then to construct Caps2NE from the data and to learn model parameters. We finally present how Caps2NE infers embeddings for unseen nodes as well as discuss its advantage over the GCN-based graph embedding models.

**Definition 1.** A network graph  $\mathcal{G}$  is defined as  $\mathcal{G} = (\mathcal{V}, \mathcal{E})$ , in which  $\mathcal{V}$  is a set of nodes and  $\mathcal{E} \subseteq \{(v, v') | v, v' \in \mathcal{V}\}$  is a set of edges. A graph embedding model aims to learn a node embedding  $\mathbf{o}_v$  for each node  $v \in \mathcal{V}$ .

**Sampling an input.** We follow [23] to uniformly sample a number  $T$  of random walks of length  $q$  for every node in  $\mathcal{V}$ . From each walk, we randomly sample a target node  $v$  and treat  $(q - 1)$  remaining nodes in the walk as the context nodes in order to construct an input pair of  $(C_v, v)$ . We denote  $C_v$  be the list of context nodes  $v_i$  of the target node  $v$  (here,  $i \in \{1, 2, \dots, q - 1\}$  and  $|C_v| = q - 1$ ).

Figure 1 shows an example of a graph consisting of 6 nodes. If we sample a random walk of length  $q = 6$  for node 1 such as  $\{1, 2, 3, 4, 5, 6\}$  and select node 3 as the target node  $v$ , then remaining nodes  $\{1, 2, 4, 5, 6\}$  are treated as the context nodes of node 3, i.e.  $C_v = \{v_1 = 1, v_2 = 2, v_3 = 4, v_4 = 5, v_5 = 6\}$ .

**Definition 2.** A *capsule* is a group of neurons. A *capsule layer* is a group of capsules without connections among capsules in the same layer [24]. Two continuous layer is connected using a *routing process*.

**Constructing the proposed Caps2NE.** We build our Caps2NE with two capsule layers: In the first layer, we construct  $(q - 1)$  capsules, where each feature-based output vector of a context node  $v_i$  is encapsulated by the  $i^{th}$  corresponding capsule ( $i \in \{1, 2, \dots, q - 1\}$ ). In the second layer, we construct one capsule which produces a vector output used to infer an embedding for the target node  $v$ .

The first capsule layer consists of  $(q - 1)$  capsules, in which each  $i^{th}$  capsule outputs a vector  $\mathbf{u}_{v_i}^{(i)} \in \mathbb{R}^d$  that is computed based on a feature vector  $\mathbf{x}_{v_i} \in \mathbb{R}^d$  of the context node  $v_i$ , using a non-linear squashing function as follows:

$$\mathbf{u} = \text{squash}(\mathbf{x}) = \frac{\|\mathbf{x}\|^2}{1 + \|\mathbf{x}\|^2} \frac{\mathbf{x}}{\|\mathbf{x}\|} \quad (1)$$

Depending on the experimental dataset, input feature vectors  $\mathbf{x}_{v_i}$  in the first capsule layer are either pre-computed or randomly initialized. The squashing function ensures that the orientation of each feature vector is unchanged while its length is scaled down to below 1, i.e.,  $\mathbf{u} \in \mathbb{R}^d$  and  $\|\mathbf{u}\| < 1$ .

Vectors  $\mathbf{u}_{v_i}^{(i)}$  are linearly transformed using weight matrices  $\mathbf{W}_i \in \mathbb{R}^{k \times d}$  to produce vectors  $\hat{\mathbf{u}}_{v_i}^{(i)} \in \mathbb{R}^k$ . These vectors  $\hat{\mathbf{u}}_{v_i}^{(i)}$  are summed to result in an input vector  $\mathbf{s}_v \in \mathbb{R}^k$  for the capsule in the second layer (recall that the second layer consists of only one capsule). This capsule then performs the non-linear squashing function to output a vector  $\mathbf{e}_v \in \mathbb{R}^k$ . Formally, we have:

$$\mathbf{e}_v = \text{squash}(\mathbf{s}_v) ; \mathbf{s}_v = \sum_i c_i \hat{\mathbf{u}}_{v_i}^{(i)} ; \hat{\mathbf{u}}_{v_i}^{(i)} = \mathbf{W}_i \mathbf{u}_{v_i}^{(i)} \quad (2)$$

where  $c_i$  are coupling coefficients determined by the routing process as presented in Algorithm 1. Here,  $c_i$  helps weight the output vector  $\mathbf{u}_{v_i}^{(i)}$  of the  $i^{th}$  capsule in the first layer.

*Operating in the routing process:* As we use one capsule in the second layer, we make two differences in our routing process in Algorithm 1: (i) we apply softmax in a direction from all capsules in the previous layer to each of capsules in the next layer, (ii) we propose the use of a new update rule ( $b_i \leftarrow \hat{\mathbf{u}}_{v_i}^{(i)} \cdot \mathbf{e}_v$ ) instead of employing ( $b_i \leftarrow b_i + \hat{\mathbf{u}}_{v_i}^{(i)} \cdot \mathbf{e}_v$ ) originally used by [24].

---

**Algorithm 1:** The Caps2NE routing process.

---

```

1 for  $i = 1, 2, \dots, q-1$  do
2    $b_i \leftarrow 0$ 
3 for iteration = 1, 2, ...,  $m$  do
4    $\mathbf{c} \leftarrow \text{softmax}(\mathbf{b})$ 
5    $\mathbf{s}_v \leftarrow \sum_i c_i \hat{\mathbf{u}}_{v_i}^{(i)}$ 
6    $\mathbf{e}_v \leftarrow \text{squash}(\mathbf{s}_v)$ 
7   for  $i = 1, 2, \dots, q-1$  do
8      $b_i \leftarrow \hat{\mathbf{u}}_{v_i}^{(i)} \cdot \mathbf{e}_v$ 

```

---

**Learning parameters of Caps2NE.** The output vector  $\mathbf{e}_v$  is finally used to infer the embedding  $\mathbf{o}_v$  of the target node  $v$ , as learned via Equation 3. We learn all model parameters (including the node embeddings  $\mathbf{o}_v$ ) by minimizing the sampled softmax loss function [13]

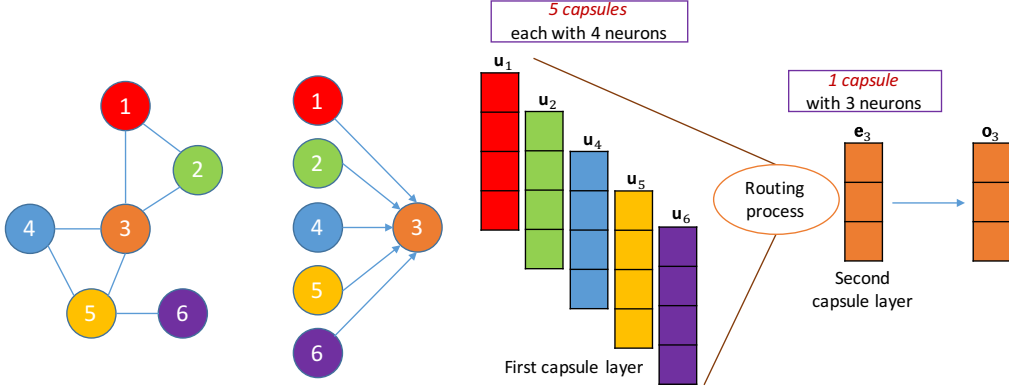


**Figure 1:** Processes in our Caps2NE with  $q = 6, d = 4, k = 3$  for an illustration purpose. Note that in this illustration, we use numbered subscripts to denote nodes themselves, not indexes of nodes or capsules. The indexes of capsules are fixed from 1 to  $(q - 1)$ , not depending on the indexes of the context nodes. With  $v$  be the target node 3, we have  $C_v = \{v_1 = 1, v_2 = 2, v_3 = 4, v_4 = 5, v_5 = 6\}$ .

applied to the target node  $v$  as follows:

$$\mathcal{L}_{\text{Caps2NE}}(v) = -\log \frac{\exp(\mathbf{o}_v^T \mathbf{e}_v)}{\sum_{v' \in \mathcal{V}'} \exp(\mathbf{o}_v^T \mathbf{e}_{v'})} \quad (3)$$

where  $\mathcal{V}'$  is a subset sampled from  $\mathcal{V}$ .

---

**Algorithm 2:** The Caps2NE learning process within each training epoch.

---

- 1 **Input:** A network graph  $\mathcal{G} = (\mathcal{V}, \mathcal{E})$
  - 2 **for**  $v \in \mathcal{V}$  **do**
  - 3     SAMPLE  $T$  random walks of length  $q$  starting at  $v$
  - 4 **for** each random walk **do**
  - 5     SAMPLE a node  $v$  as a target node
  - 6      $C_v \leftarrow$  Remaining nodes
  - 7     **for**  $i = 1, 2, \dots, q-1$  **do**
  - 8          $\mathbf{u}_{v_i}^{(i)} \leftarrow \text{squash}(\mathbf{x}_{v_i}) \quad \forall v_i \in C_v$
  - 9      $\mathbf{e}_v \leftarrow \text{ROUTING} \left( \left\{ \mathbf{u}_{v_i}^{(i)} \right\}_{i=1}^{q-1} \right)$
  - 10     $\mathbf{o}_v \leftarrow \mathbf{e}_v$
- 

We briefly represent the general learning process of our proposed Caps2NE model in Algorithm 2 whose main steps **3**, **7-9** and **10** are previously detailed in parts “*Sampling an input*”, “*Constructing the proposed Caps2NE*” and “*Learning parameters of Caps2NE*”, respectively.

**Illustrating Caps2NE.** We illustrate our proposed model in Figure 1 where the length  $q$  of random walks, the dimensional size  $d$  of input feature vectors and the dimensional size  $k$  of output node embeddings are equal to 6, 4 and 3, respectively. Thus, the first capsule layer has 5 capsules, each with 4 neurons, and the second capsule layer has 1 capsule with 3 neurons. For the target node 3 in the illustration, the vector output of the capsule in the second layer is used to infer the embedding of node 3. Our Caps2NE can directly aggregate feature information from nodes at many hops away on random walks (e.g., directly aggregating the information from context node 6 to target node 3), so this helps our model to effectively infer the plausible embeddings for new nodes.

**Inferring embeddings for new nodes in the inductive setting.** Algorithm 3 shows how we infer an embedding for a new node  $v$  given

---

**Algorithm 3:** The inference process for new nodes.

---

- 1 **Input:** A network graph  $\mathcal{G} = (\mathcal{V}, \mathcal{E})$ , a trained model Caps2NE<sub>trained</sub>, a set  $\mathcal{V}_{\text{test}}$  of new nodes.
  - 2 **for**  $v \in \mathcal{V}_{\text{test}}$  **do**
  - 3     SAMPLE  $Z$  pairs  $\{p_j\}_{j=1}^Z$  of  $(C_v, v)$
  - 4     **for**  $j \in \{1, 2, \dots, Z\}$  **do**
  - 5          $\mathbf{e}_{(v,j)} \leftarrow \text{Caps2NE}_{\text{trained}}(p_j)$
  - 6      $\mathbf{o}_v \leftarrow \text{AVERAGE}(\{\mathbf{e}_{(v,j)}\}_{j=1}^Z)$
- 

an existing graph. After training our model, we generate random walks of length  $q$  to extract  $Z$  pairs of  $(C_v, v)$ . We use each of these pairs as an input for our trained model and then collect the output vector  $\mathbf{e}$  from the second capsule layer. Thus, we obtain  $Z$  vectors associated with node  $v$  and then average them into an embedding representation of  $v$ .

**Comparing Caps2NE with GCN-based models.** The GCN-based architecture is fixed for each particular graph, so we cannot attach nodes to different contexts. In order to bypass this, we have to build multiple layers stacked on top of each other. For example, as shown in Figure 1, if we want to aggregate the information from node 1 to node 6 using such a stacked model as GCN or GAT, we have to build at least 4 GCN/GAT layers, in order to transfer the information from node 1 at the first layer to node 3 at the second layer, then to node 5 at the third layer, and finally to node 6 at the fourth layer. This example implies an indirect transfer of the aggregation process in the GCN-based models. In addition, directly integrating our inference process into the GCN-based models is not easy. As a result, the GCN-based models encounter a propagation issue of inferring the plausible embeddings for new nodes, especially when the neighbors of a new node are also unseen during training.

### 3 Experimental setup

We conduct experiments to evaluate our Caps2NE on the node classification task: (i) We unsupervisedly train Caps2NE to obtain node embeddings. (ii) We use the obtained node embeddings as feature vectors to train a logistic regression classifier for predicting node labels. (iii) We evaluate Caps2NE using well-known benchmark datasets with and without using pre-computed node features, and then also analyze effects of hyper-parameters.

### 3.1 Datasets

Table 1 presents the statistics of six experimental datasets that we use for evaluation:

- CORA, CITESEER [25] and PUBMED [21] are citation networks where each node represents a document (here, each node is associated with a class labeling the main topic of the document) and each edge represents a citation link between two documents. Each node is also associated with a “pre-computed” vector of a bag-of-words, i.e. the input feature vectors  $\mathbf{x}_{v_i}$  in the first capsule layer (Equation 1) are pre-computed based on bag-of-words features and fixed during training.
- PPI [3] is a subgraph of the Protein-Protein Interaction network for Homo Sapiens, and its node labels represent biological states. POS [19] is a co-occurrence network of words from the Wikipedia dump, and its node labels represent the part-of-speech tags. BLOGCATALOG [32] is a social network of relationships of the bloggers listed on the BlogCatalog website, and its node labels represent bloggers’ interests. PPI, POS and BLOGCATALOG are given without node features, in which each node is assigned with one or more class labels. These datasets are used for the multi-label node classification task.

Following previous works, CORA, CITESEER and PUBMED are used in both the transductive and inductive settings, while PPI, POS and BLOGCATALOG are used in the transductive setting.

**Table 1:** Statistics of the experimental datasets. #L denotes the number of node labels (classes).  $d$  is the dimensional size of the input “pre-computed” feature vectors  $\mathbf{x}_{v_i}$  in the first capsule layer ( $\mathbf{x}_{v_i}$  is fixed during training). For the last 3 rows, the feature vectors  $\mathbf{x}_{v_i}$  are randomly initialized and then updated during training.

Dataset	$ \mathcal{V} $	$ \mathcal{E} $	#L	$d$
CORA	2,708	5,429	7	1,433
CITESEER	3,327	4,732	6	3,703
PUBMED	19,717	44,338	3	500
PPI	3,890	76,584	50	–
POS	4,777	184,812	40	–
BLOGCATALOG	10,312	333,983	39	–

### 3.2 Data splits for the node classification task

**PPI, POS and BLOGCATALOG.** A certain fraction  $\gamma$  of nodes is provided to train a classifier which is then used to predict the labels of the remaining nodes.

**CORA, CITESEER and PUBMED.** [7] show that the experimental setup used in [15, 27] is not fair to show the effectiveness of existing models when these models are evaluated using the fixed & pre-split training, validation and test sets from the Planetoid model [30]. Therefore, for a fair comparison, we follow the experimental setup of [7]. In particular, on each experimental dataset, we uniformly sample 20 random nodes for each class as training data, 1000 different random nodes as a validation set and 1000 different random nodes as a test set. We then repeat this manner 10 times to produce 10 training-validation-test data splits to each of the experimental datasets.

### 3.3 Training protocol to learn node embeddings

There are hyper-parameters that could affect final results, e.g., the walk length  $q$ , the embedding size  $k$  or the number  $Z$  of pairs in

Algorithm 3. We could improve obtained results by carefully tuning such hyper-parameters, but this is not central point of our paper. The objective of this paper is to investigate whether capsules can effectively capture graph structures of data, resulting in competitive performances for the node classification task. We thus only tune the Adam initial learning rate  $lr$ , the number  $T$  of random walks and the number  $m$  of iterations in the routing process (Algorithm 1).

**PPI, POS and BLOGCATALOG:** We only use the transductive setting for these three datasets. We uniformly sample 64 random walks ( $T = 64$ ) of length 10 ( $q = 10$ ) for each node in the graph. In each random walk, we rotationally select each node in the walk as a target node and 9 remaining nodes as its context nodes. We also run up to 50 training epochs and use the batch size to 128, the embedding size  $k = 128$  and  $|\mathcal{V}'| = 256$  in Equation 3. We vary the Adam initial learning rate  $lr \in \{1e^{-5}, 5e^{-5}, 1e^{-4}\}$ . Nodes are given without pre-computed features, hence we set the size  $d$  of feature vectors  $\mathbf{x}_{v_i}$  to 128 ( $d = 128$ ), and these vectors are randomly initialized uniformly, and updated during training.

**CORA, CITESEER and PUBMED:**

**Transductive setting.** We train Caps2NE using the entire input graph, i.e., all nodes are present when training. We set the embedding size  $k$  to 128 ( $k = 128$ ) and the number of samples in the sampled softmax loss function to 256 ( $|\mathcal{V}'| = 256$  in Equation 3). We also set the batch size to 64 for both CORA and CITESEER and to 128 for PUBMED. In preliminary experiments, using the long walk lengths ( $q \in \{20, 30\}$ ) produces a similar performance to using a shorter walk length ( $q = 10$ ). Thus, we use a fixed walk length  $q = 10$  for uniformly sampling  $T$  random walks starting from each node. We also rotationally select each node in the walk as a target node and 9 remaining nodes as its context nodes. Therefore, we only select target nodes at indexes of  $\{3, 4, 5, 6\}$ . We optimize the loss function using Adam [14], and apply a grid search to select the Adam initial learning rate  $lr \in \{1e^{-5}, 5e^{-5}, 1e^{-4}\}$ , the number  $T$  of random walks  $T \in \{8, 16, 32, 64\}$  and the number  $m$  of iterations in the routing process (Algorithm 1)  $m \in \{1, 3, 5, 7\}$ . We run up to 50 epochs and evaluate the model on each epoch to choose the best model on the validation set (See details in Evaluation protocol). We use the same values of hyper-parameters above for every data split.

**Inductive setting.** We use the same inductive setting as in [30, 7]: We firstly remove all nodes in the test set from the original graph before training phase, thus these nodes are unseen/new in the testing/evaluating phase. We then apply the standard training process on the remaining of the graph. Here, we use the same set of hyper-parameters tuned for the transductive setting to train Caps2NE in the inductive setting. After training, we infer the embedding for each node  $v$  in the test set as in Algorithm 3 using a fixed value  $Z = 10$ .

### 3.4 Evaluation protocol

**PPI, POS and BLOGCATALOG.** We follow the same experimental setup used for the multi-label node classification task from [23] and [7]: We uniformly sample a fraction  $\gamma$  of nodes at random as training set for learning a one-vs-rest logistic regression classifier. The learned node embeddings after each Caps2NE training epoch are used as input feature vectors for this logistic regression classifier. We use default parameters for learning this classifier from [23]. The classifier is then used to categorize the remaining nodes. We monitor the Micro-F1 and Macro-F1 scores of the classifier after each Caps2NE training epoch, for which the best model is chosen by using 10-fold cross-validation for each fraction value. We repeat this manner 10

**Table 2:** Multi-label classification results on PPI, POS and BLOGCATALOG. Baseline results are from [7].

Method (Micro-F1)	POS			PPI			BLOGCATALOG		
	$\gamma = 10\%$	$\gamma = 50\%$	$\gamma = 90\%$	$\gamma = 10\%$	$\gamma = 50\%$	$\gamma = 90\%$	$\gamma = 10\%$	$\gamma = 50\%$	$\gamma = 90\%$
DeepWalk	45.02	49.10	49.33	17.14	<b>23.52</b>	25.02	34.48	38.11	38.34
LINE	45.22	<b>51.64</b>	<u>52.28</u>	16.55	23.01	<b>25.28</b>	34.83	38.99	38.77
Node2Vec	44.66	48.73	49.73	17.00	<u>23.31</u>	24.75	<b>35.54</b>	<u>39.31</u>	40.03
EP-B	<b>46.97</b>	49.52	50.05	<u>17.82</u>	23.30	24.74	<u>35.05</u>	<b>39.44</b>	<u>40.41</u>
Our Caps2NE	<u>46.01</u>	<u>50.93</u>	<b>53.92</b>	<b>18.52</b>	23.15	<u>25.08</u>	34.31	38.35	<b>40.79</b>

Method (Macro-F1)	POS			PPI			BLOGCATALOG		
	$\gamma = 10\%$	$\gamma = 50\%$	$\gamma = 90\%$	$\gamma = 10\%$	$\gamma = 50\%$	$\gamma = 90\%$	$\gamma = 10\%$	$\gamma = 50\%$	$\gamma = 90\%$
DeepWalk	8.20	10.84	12.23	13.01	18.73	20.01	18.16	22.65	22.86
LINE	8.49	<u>12.43</u>	<u>12.40</u>	12.79	18.06	<b>20.59</b>	18.13	22.56	23.00
Node2Vec	8.32	11.07	12.11	13.32	18.57	19.66	<b>19.08</b>	23.97	24.82
EP-B	<u>8.85</u>	10.45	12.17	<u>13.80</u>	<u>18.96</u>	<u>20.36</u>	<b>19.08</b>	<b>25.11</b>	<u>25.97</u>
Our Caps2NE	<b>9.71</b>	<b>13.16</b>	<b>14.11</b>	<b>15.20</b>	<b>19.63</b>	20.27	<u>18.40</u>	<u>24.80</u>	<b>26.63</b>

times for each fraction value, and then compute the averaged Micro-F1 and Macro-F1 scores. We show final scores w.r.t. each value  $\gamma \in \{10\%, 50\%, 90\%\}$ . The baseline graph embedding models on POS, PPI and BLOGCATALOG are DeepWalk, LINE, Node2Vec and EP-B.

**CORA, CITESEER and PUBMED.** We also follow the same setup that [7] use to evaluate their EP-B model w.r.t. the multi-class node classification task. For each of 10 training-validation-test data splits, the learned node embeddings after each Caps2NE training epoch are used as feature vectors for learning a L2-regularized logistic regression classifier on the training set.<sup>5</sup> We monitor the node classification accuracy on the validation set for every Caps2NE training epoch, and take the model that helps the logistic regression classifier producing the highest accuracy on the validation set to compute the accuracy on the test set. We finally report the average of the accuracies over 10 test sets in the 10 data splits. We compare Caps2NE with strong graph embedding baselines BoW (Bag-of-Words), DeepWalk, DeepWalk+BoW, EP-B, Planetoid, GCN and GAT. As reported in [10], GraphSAGE obtained low accuracies on CORA, PUBMED and CITESEER, thus we do not include GraphSAGE as a strong baseline.

## 4 Experimental results

### 4.1 Overall results

**PPI, POS and BLOGCATALOG.** We show in Table 2 the Micro-F1 and Macro-F1 scores on test sets in the transductive setting. Especially, on POS, Caps2NE produces a new state-of-the-art Macro-F1 score for each of the three fraction values  $\gamma$ , the highest Micro-F1 score when  $\gamma = 90\%$  and the second highest Micro-F1 scores when  $\gamma \in \{10\%, 50\%\}$ . Caps2NE obtains new highest F1 scores on PPI and BLOGCATALOG when  $\gamma = 10\%$  and  $\gamma = 90\%$ , respectively. On PPI, Caps2NE also achieves the highest Macro-F1 score when  $\gamma = 50\%$  and the second highest Micro-F1 score when  $\gamma = 90\%$ . On BLOGCATALOG, Caps2NE also achieves the second highest Macro-F1 scores when  $\gamma \in \{10\%, 50\%\}$ .

In short, from Table 2, Caps2NE obtains top performances on these three datasets: producing the highest scores in 9 over 18 comparison groups (3 datasets  $\times$  3 values of the fraction  $\gamma \times$  2 metrics), the second highest scores in 5/18 groups and competitive scores in the remaining 4 groups.

<sup>5</sup> We use the logistic regression classifier from LIBLINEAR [8], and set tolerance of termination criterion to 0.001.

**Table 3:** Accuracies on the CORA, CITESEER and PUBMED test sets in the transductive and inductive settings. “Un-sup.” denotes unsupervised graph embedding models, where the best score is in bold while the second best score is in underline. “Sup.” denotes supervised graph embedding models that additionally use node labels when training the models.

		Transductive	CORA	CITESEER	PUBMED
Un-sup.	BoW		58.63	58.07	70.49
	DeepWalk		71.11	47.60	73.49
	DeepWalk+BoW		76.15	61.87	77.82
	EP-B		<u>78.05</u>	<u>71.01</u>	<b>79.56</b>
	Our Caps2NE		<b>80.53</b>	<b>71.34</b>	78.45
Sup.	GAT		81.72	70.80	79.56
	GCN		79.59	69.21	77.32
	Planetoid		71.90	58.58	74.49
		Inductive	CORA	CITESEER	PUBMED
Un-sup.	DeepWalk+BoW		68.35	59.47	74.87
	EP-B		<u>73.09</u>	<u>68.61</u>	<b>79.94</b>
	Our Caps2NE		<b>76.54</b>	<b>69.84</b>	<u>78.98</u>
Sup.	GAT		69.37	59.55	71.29
	GCN		67.76	63.40	73.47
	Planetoid		64.80	61.97	75.73

**CORA, CITESEER and PUBMED.** Table 3 reports the experimental results in the transductive and inductive settings. BoW is evaluated by directly using the pre-computed bag-of-words feature vectors for learning the classifier, thus its performance is the same for both settings. DeepWalk+BoW concatenates the learned embedding of a node from DeepWalk with the pre-computed BoW feature vector of the node. As discussed in [7], the experimental setup used to evaluate GCN and GAT is not fair for existing models when they are evaluated using the fixed & pre-split training, validation and test sets from [30]. Thus we report results, and also fine-tune and re-evaluate GAT, using the same experimental setup used in [7]. The results of other baselines (e.g., BoW, DeepWalk+BoW, EP-B, Planetoid and GCN) are taken from [7].

**Transductive setting:** Under the transductive setting, Caps2NE obtains the highest scores on CORA and CITESEER and the second highest score on PUBMED against other unsupervised baseline models. In addition, we also compare our unsupervised Caps2NE to the advanced supervised models GCN, Planetoid and GAT: Caps2NE works better than GCN and Planetoid on these three datasets, and outperforms GAT on CITESEER.

**Inductive setting:** Table 3 also shows that under the inductive

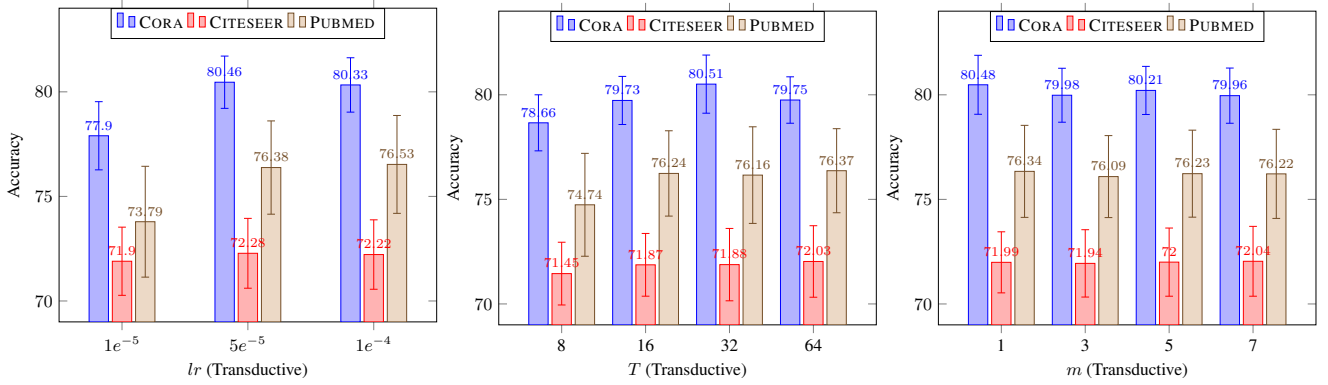


**Figure 2:** Effects of the Adam initial learning rate  $lr$  (left figure), the number  $T$  of random walks sampled for each node (central figure), and the number  $m$  of iterations in the routing process (right figure) on the validation sets in the transductive setting.

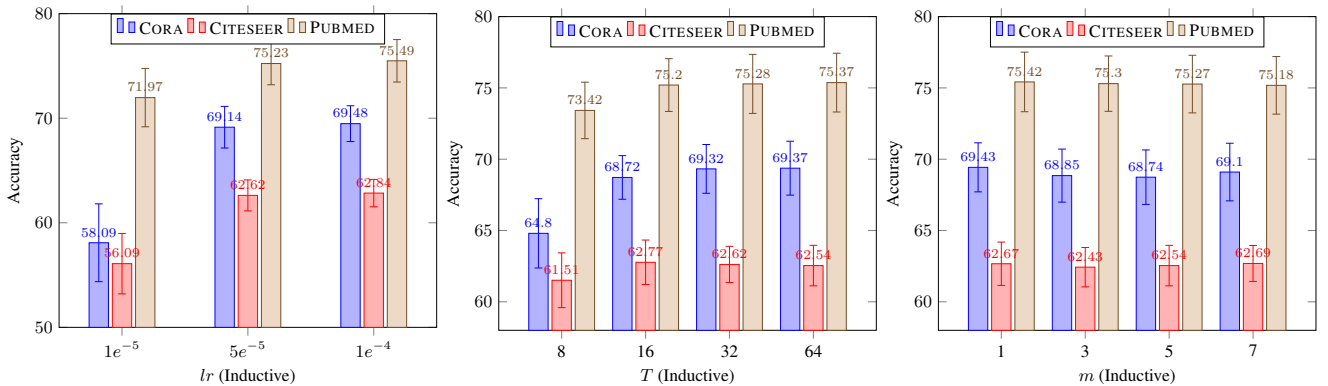


**Figure 3:** Effects of the Adam initial learning rate  $lr$  (left figure), the number  $T$  of random walks sampled for each node (central figure), and the number  $m$  of iterations in the routing process (right figure) on the validation sets in the inductive setting.

setting, Caps2NE produces new state-of-the-art scores of 76.54% and 69.84% on CORA and CITESEER respectively, and also obtains the second highest score of 78.98% on PUBMED. As previously discussed in the last paragraph in the “The proposed Caps2NE” section, we re-emphasize that our unsupervised Caps2NE model notably outperforms the supervised models GCN and GAT for this inductive setting. In particular, Caps2NE achieves 4+% absolute higher accuracies than both GCN and GAT on the three datasets, clearly showing the effectiveness of Caps2NE to infer embeddings for unseen nodes.

EP-B is the current best model on PUBMED: (i) EP-B also simultaneously learns word embeddings on texts from all nodes. Then the embeddings of words associated to each node are averaged into a new feature vector which is then used to reconstruct the node embedding. (ii) On PUBMED, neighbors of unseen nodes in the test set are frequently unseen in the training set. Therefore, these (i) and (ii) are reasons why on PUBMED, EP-B obtains higher performance than Caps2NE and other models (here, we only make use of the “pre-computed” bag-of-words feature vectors).

## 4.2 Effects of hyper-parameters

Figures 2 and 3 present effects of the Adam initial learning rate  $lr$ , the number  $T$  of random walks sampled for each node and the number  $m$  of iterations in the routing process on the validation sets in the transductive and inductive settings respectively. In these experiments, for all 10 data splits, we apply the same value of one hyper-parameter and then tune other hyper-parameters.

**Table 4:** The best configurations of hyper-parameters  $T$  and  $m$  for the transductive and inductive settings on the validation set in each data split.

Split	Transductive						Inductive					
	CORA		CITESEER		PUBMED		CORA		CITESEER		PUBMED	
	$T$	$m$	$T$	$m$	$T$	$m$	$T$	$m$	$T$	$m$	$T$	$m$
1st	32	1	16	7	16	3	32	1	64	7	64	1
2nd	32	1	8	5	32	1	32	1	16	1	32	1
3rd	32	1	64	7	64	7	64	7	32	7	64	1
4th	32	1	64	3	16	5	32	1	16	7	64	5
5th	32	1	32	5	64	7	64	1	32	1	32	1
6th	16	1	16	5	16	7	32	1	64	1	16	1
7th	32	1	8	1	64	5	64	1	64	5	32	1
8th	32	1	16	7	16	1	64	1	16	7	64	3
9th	32	1	64	1	32	1	64	7	16	1	64	1
10th	32	5	32	5	16	7	32	3	16	5	16	3

We find that in general using  $lr = 1e^{-4}$  produces the top scores on the validation sets to both transductive and inductive settings. We also find that we generally obtain high accuracies with a high value of  $T$  at either 32 or 64. However, there is an exception in the inductive setting, where using  $T = 16$  produces the highest accuracy on CITESEER. A possible reason might come from the fact that CITESEER is more sparse than CORA and PUBMED: the average number of neighbors per node on CITESEER is 1.4 which is substantially smaller than 2.0 on CORA and 2.2 on PUBMED.

When it comes to  $m$ , in the inductive setting, using  $m = 1$  obtains the top performances. In addition, in the transductive setting, using  $m = 1$  also obtains the highest accuracy on CORA. Note that the best configurations of hyper-parameters over 10 data splits are not always

**Table 5:** Accuracy results on the CORA validation sets w.r.t each data split and each value  $m > 1$  of routing iterations for the transductive and inductive settings. Regarding Algorithm 1 when  $m > 1$ , ‘‘Ours’’ denotes our update rule ( $b_i \leftarrow \hat{\mathbf{u}}_i^{(i)} \cdot \mathbf{e}_v$ ), while ‘‘Sab.’’ denotes the update rule ( $b_i \leftarrow b_i + \hat{\mathbf{u}}_i^{(i)} \cdot \mathbf{e}_v$ ) originally used by [24].

Split	Transductive						Inductive					
	$m=3$		$m=5$		$m=7$		$m=3$		$m=5$		$m=7$	
	Ours	Sab.	Ours	Sab.	Ours	Sab.	Ours	Sab.	Ours	Sab.	Ours	Sab.
1st	80.1	80.1	80.2	79.6	79.7	79.3	70.2	70.3	70.2	69.2	70.6	68.3
2nd	79.4	79.6	79.7	78.9	79.7	78.6	66.0	65.9	65.7	64.4	65.6	64.3
3rd	78.5	78.5	78.6	78.6	78.5	78.4	68.2	67.6	68.3	68.4	69.2	67.6
4th	81.3	80.8	81.1	80.1	81.1	79.3	66.5	66.3	66.5	65.4	66.4	65.9
5th	81.9	81.6	81.7	81.5	81.7	80.9	69.4	68.7	69.9	68.5	69.5	68.1
6th	78.6	79.0	78.8	78.7	78.7	78.0	66.7	67.1	66.7	66.2	67.5	65.3
7th	80.1	80.2	80.5	80.0	79.9	79.4	70.4	70.1	70.4	69.9	70.4	68.8
8th	81.8	82.1	82.1	81.5	82.3	81.2	69.6	69.0	68.7	67.8	69.7	67.5
9th	79.3	79.4	79.7	78.1	78.6	77.8	71.2	70.8	71.5	71.7	72.2	70.1
10th	78.8	79.3	79.7	78.9	79.4	78.7	70.3	69.7	69.5	68.8	69.9	68.3
Overall	79.98	<b>80.06</b>	<b>80.21</b>	79.59	<b>79.96</b>	79.16	<b>68.85</b>	68.55	<b>68.74</b>	68.03	<b>69.10</b>	67.42

relied on using  $m = 1$  as shown in Table 4.

### 4.3 Ablation analysis on the routing update

The routing process presented in Algorithm 1 can be considered as an attention mechanism to compute the coupling coefficient  $c_i$  which is used to weight the output of the  $i^{th}$  capsule in the first layer. [24] use ( $b_i \leftarrow b_i + \hat{\mathbf{u}}_i^{(i)} \cdot \mathbf{e}_v$ ) for the image classification task, but this might not be well-suited for graph-structured data because of the high order variant among different nodes. Therefore, we propose to use the new update rule ( $b_i \leftarrow \hat{\mathbf{u}}_i^{(i)} \cdot \mathbf{e}_v$ ) as this new rule generally helps obtain a higher performance for each setup. Table 5 shows a comparison between the accuracy results of these two update rules on the CORA validation sets w.r.t each data split and each value  $m > 1$  of routing iterations.

### 4.4 Effects of capsules on node orders

Node orders in the generated random walks partially reflect the graph structures. Therefore, we investigate whether capsules can capture the graph structures when re-ordering the nodes in the random walks. We use the same random walks generated for CORA, CITESEER and PUBMED in the transductive setting, but we now apply an additional step of shuffling context nodes when training Caps2NE, i.e., re-ordering nodes to find out whether capsules can still model graph structures effectively. We perform the same training and evaluation protocols as did previously.

We obtain the average accuracy results of 80.52%, 72.28% and 76.53% in using the additional shuffling step, which are similar to accuracies of 80.56%, 72.29% and 76.60% from the original training protocol (i.e., without using the shuffling step) over the CORA, CITESEER and PUBMED validation sets from 10 data splits, respectively. We also apply t-SNE [18] to visualize node embeddings learned by Caps2NE on PUBMED in Figure 4. We find that there is a similarity in the learned node embeddings between with and without using the shuffling step. These imply that capsules can still capture graph structures to achieve top performances when reordering the nodes in the random walks.

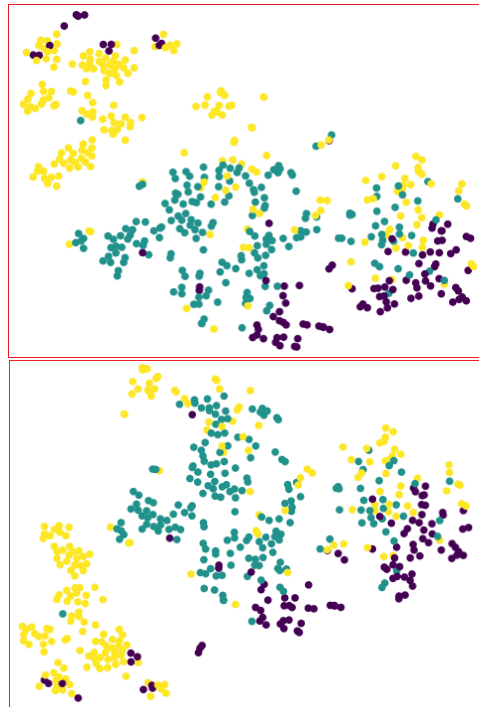


**Figure 4:** Visualization of learned node embeddings on PUBMED. Colors denote classes. i) Top picture: with using the shuffling step. ii) Bottom picture: without using the shuffling step.

## 5 Conclusions and future work

In this paper, we have presented the new unsupervised embedding model Caps2NE based on the capsule network to learn node embeddings from the graph-structured data. Our proposed model Caps2NE can effectively use context nodes at many hops away on random walks to infer plausible embeddings for target nodes. Experimental results show that Caps2NE obtains the top performances on six benchmark datasets for the node classification task. In the future work, we plan to extend Caps2NE with a supervised manner to achieve better performances. Our code is available at: <https://anonymous-url/>.

## REFERENCES

- [1] Dzmitry Bahdanau, Kyunghyun Cho, and Yoshua Bengio, 'Neural machine translation by jointly learning to align and translate', in *ICLR*, (2015).
- [2] Peter W Battaglia, Jessica B Hamrick, Victor Bapst, Alvaro Sanchez-Gonzalez, Vinicius Zambaldi, Mateusz Malinowski, Andrea Tacchetti, David Raposo, Adam Santoro, Ryan Faulkner, et al., 'Relational inductive biases, deep learning, and graph networks', *arXiv preprint arXiv:1806.01261*, (2018).
- [3] Bobby-Joe Breitkreutz, Chris Stark, Teresa Reguly, Lorrie Boucher, Ashton Breitkreutz, Michael Livstone, Rose Oughtred, Daniel Lackner, Jrg Bhler, Valerie Wood, Kara Dolinski, and Mike Tyers, 'The BioGRID interaction database: 2008 update', *Nucleic acids research*, **36**, D637–40, (2008).
- [4] Hongyun Cai, Vincent W Zheng, and Kevin Chang, 'A comprehensive survey of graph embedding: problems, techniques and applications', *IEEE Transactions on Knowledge and Data Engineering*, **30**, 1616–1637, (2018).
- [5] Haochen Chen, Bryan Perozzi, Rami Al-Rfou, and Steven Skiena, 'A tutorial on network embeddings', *arXiv preprint arXiv:1808.02590*, (2018).
- [6] Zhiyong Cui, Kristian Henrickson, Ruimin Ke, and Yinhai Wang, 'High-order graph convolutional recurrent neural network: A deep learning framework for network-scale traffic learning and forecasting', *arXiv preprint arXiv:1802.07007*, (2018).
- [7] Alberto Garcia Duran and Mathias Niepert, 'Learning Graph Representations with Embedding Propagation', in *NIPS*, pp. 5119–5130, (2017).
- [8] Rong-En Fan, Kai-Wei Chang, Cho-Jui Hsieh, Xiang-Rui Wang, and Chih-Jen Lin, 'LIBLINEAR: A Library for Large Linear Classification', *Journal of Machine Learning Research*, **9**, 1871–1874, (2008).
- [9] Aditya Grover and Jure Leskovec, 'Node2Vec: Scalable Feature Learning for Networks', in *SIGKDD*, pp. 855–864, (2016).
- [10] Junliang Guo, Linli Xu, and Enhong Chen, 'Spine: Structural identity preserved inductive network embedding', *arXiv preprint arXiv:1802.03984*, (2018).
- [11] William L. Hamilton, Rex Ying, and Jure Leskovec, 'Inductive representation learning on large graphs', in *NIPS*, pp. 1024–1034, (2017).
- [12] William L. Hamilton, Rex Ying, and Jure Leskovec, 'Representation learning on graphs: Methods and applications', *arXiv preprint arXiv:1709.05584*, (2017).
- [13] Sébastien Jean, Kyunghyun Cho, Roland Memisevic, and Yoshua Bengio, 'On using very large target vocabulary for neural machine translation', in *ACL*, pp. 1–10, (2015).
- [14] Diederik Kingma and Jimmy Ba, 'Adam: A method for stochastic optimization', *arXiv preprint arXiv:1412.6980*, (2014).
- [15] Thomas N. Kipf and Max Welling, 'Semi-Supervised Classification with Graph Convolutional Networks', in *ICLR*, (2017).
- [16] Y. LeCun, B. Boser, J. S. Denker, D. Henderson, R. E. Howard, W. Hubbard, and L. D. Jackel, 'Backpropagation Applied to Handwritten Zip Code Recognition', *Neural Comput.*, **1**(4), 541–551, (1989).
- [17] Juzheng Li, Jun Zhu, and Bo Zhang, 'Discriminative Deep Random Walk for Network Classification', in *ACL*, pp. 1004–1013, (2016).
- [18] Laurens van der Maaten and Geoffrey Hinton, 'Visualizing data using t-SNE', *Journal of machine learning research*, **9**, 2579–2605, (2008).
- [19] Matt Mahoney. Large text compression benchmark. <http://www.matmahoney.net/text/text.html>, 2011.
- [20] Tomas Mikolov, Ilya Sutskever, Kai Chen, Gregory S. Corrado, and Jeffrey Dean, 'Distributed Representations of Words and Phrases and their Compositionality', in *NIPS*, pp. 3111–3119, (2013).
- [21] Galileo Mark Namata, Ben London, Lise Getoor, and Bert Huang, 'Query-driven Active Surveying for Collective Classification', in *Workshop on Mining and Learning with Graphs*, (2012).
- [22] Lawrence Page, Sergey Brin, Rajeev Motwani, and Terry Winograd, 'The PageRank citation ranking: Bringing order to the web', Technical report, Stanford InfoLab, (1999).
- [23] Bryan Perozzi, Rami Al-Rfou, and Steven Skiena, 'DeepWalk: Online Learning of Social Representations', in *SIGKDD*, pp. 701–710, (2014).
- [24] Sara Sabour, Nicholas Frosst, and Geoffrey E Hinton, 'Dynamic routing between capsules', in *NIPS*, pp. 3859–3869, (2017).
- [25] Prithviraj Sen, Galileo Namata, Mustafa Bilgic, Lise Getoor, Brian Gallagher, and Tina Eliassi-Rad, 'Collective classification in network data', *AI magazine*, **29**(3), 93, (2008).
- [26] Jian Tang, Meng Qu, Mingzhe Wang, Ming Zhang, Jun Yan, and Qiaozhu Mei, 'LINE: Large-scale Information Network Embedding', in *WWW*, pp. 1067–1077, (2015).
- [27] Petar Veličković, Guillem Cucurull, Arantxa Casanova, Adriana Romero, Pietro Liò, and Yoshua Bengio, 'Graph Attention Networks', in *ICLR*, (2018).
- [28] Daixin Wang, Peng Cui, and Wenwu Zhu, 'Structural deep network embedding', in *SIGKDD*, pp. 1225–1234, (2016).
- [29] Jizhe Wang, Pipei Huang, Huan Zhao, Zhibo Zhang, Binqiang Zhao, and Dik Lun Lee, 'Billion-scale Commodity Embedding for E-commerce Recommendation in Alibaba', in *SIGKDD*, pp. 839–848, (2018).
- [30] Zhilin Yang, William W. Cohen, and Ruslan Salakhutdinov, 'Revisiting Semi-supervised Learning with Graph Embeddings', in *ICML*, pp. 40–48, (2016).
- [31] Rex Ying, Ruining He, Kaifeng Chen, Pong Eksombatchai, William L. Hamilton, and Jure Leskovec, 'Graph Convolutional Neural Networks for Web-Scale Recommender Systems', in *SIGKDD*, pp. 974–983, (2018).
- [32] R. Zafarani and H. Liu. Social computing data repository at ASU. <http://socialcomputing.asu.edu>, 2009.
- [33] Daokun Zhang, Jie Yin, Xingquan Zhu, and Chengqi Zhang, 'Network representation learning: A survey', *IEEE Transactions on Big Data*, **to appear**, (2018).